Published in final edited form as:
Langmuir. 2011 February 15; 27(4): 1409–1414. doi:10.1021/la103961m.

Aquatic Self-Assembly of Sixteen Subunits into a 39-kDa Dendrimer

Luis R. Rivera, **José E. Betancourt**, and **José M. Rivera***
Department of Chemistry, University of Puerto Rico at Río Piedras, San Juan 00931, Puerto Rico

Abstract

We have developed the 8-(*m*-acetylphenyl)-2′-deoxyguanosine (**mAG**) scaffold for the self-assembly of supramolecules in water and for the synthesis of self-assembled dendrimers (SADs) in organic media. Previously, reported **mAG** assemblies showed promising characteristics for the construction of SADs. Yet, none of these SADs had large enough dendrons to reach a fractal geometry characteristic of high-generation dendrimers. Here we present the synthesis, as well as the molecular and supramolecular characterization of a fourth generation hydrophilic self-assembled hexadecameric dendrimer $[mAGD_4(OH)_{16}]_{16}$•3KI ($\mathbf{3}_{16}$) with a size and shape akin to globular proteins. The diameter of $\mathbf{3}_{16}$ (5.0 nm) was measured by Pulsed Field Gradient NMR and Dynamic Light Scattering experiments, which enabled the construction of a computer-generated molecular model. This SAD represents an attractive platform for biomedical applications due to its water solubility, discreteness, well defined structure, thermal stability (T_m= 68 °C), and functional core.

Introduction

Self-assembly is pivotal in the construction of naturally occurring macromolecules such as globular proteins. Their structure and function is dictated by the intertwined relationships between covalent and non-covalent interactions.[1] Synthetic macromolecules like hydrophilic dendrimers[2,3] offer a convenient platform for the development of systems with sizes and shapes similar to those of globular proteins making them suitable for biomedical applications.[4,5] The challenges imposed by the full covalent synthesis and purification of large and complex dendrimers have made of self-assembly a desirable complementary strategy.[3b] Nevertheless, the construction of biomimetic hydrophilic self-assembled dendrimers (SADs) that relies on a synergistic use of covalent and non-covalent interactions remains a tremendous challenge.

SADs constructed from biocompatible building blocks such as oligo deoxynucleotides (ODN)[6] and peptides[7,8] are viable scaffolds for selective drug transporters. Yet, the high expense and synthetic efforts to make these materials limit the amount and types of functional groups that can be incorporated into them. Furthermore, some of these strategies provide dendrimers with significant structural imperfections and polydispersity.[9]

The construction of discrete and well-defined hydrophilic SADs has been primarily limited to those whose formation is driven by coordinative bonds[10] or hydrophobic interactions.[11] Recent examples of the latter include the construction of dimeric capsular dendrimers.[12,13]

*To whom correspondence should be addressed. Telephone: 1-787-764-0000 ext. 2906 Fax: 787-756-8242. jmrivortz@mac.com..

Supporting Information Available: Detailed synthetic procedures, characterization for all new compounds, experimental protocols, and NMR data. This material is available free of charge via the Internet at http://pubs.acs.org.

Other water-soluble SADs are well defined in one dimension but ill defined in another showing a tendency to form fibers, gels, and other aggregates.[14,15] In systems that generate supramolecular objects in the nano- and micrometer scales, it is attractive to precisely control their size and shape in all dimensions.[16] Few of these strategies, rely on the combination of multiple non-covalent interactions in a programmable fashion.[15] Such strategy may also further illuminate the still imperfectly understood role of water in molecular recognition and self-assembly.[16,17]

Guanosine and related compounds have a propensity to form planar tetramers (G–tetrads) that are held together by hydrogen bonds and cation-dipole interactions (Scheme 1c). Subsequent stacking of such tetrads lead to structures known as G-quadruplexes (GQs).[18,19] Recently, we reported that the 8-(*meta*-acetylphenyl)-2′-deoxyguanosine (**mAG**) motif enables the assembly of isostructural hexadecamers in both organic[20] and aqueous media.[21] Concurrently, we developed the use of **mAG** analogues for the construction of lipophilic SADs.[22] What makes these assemblies attractive is their high fidelity and molecularity, which are consequences of a cooperative network of multiple non-covalent. The supramolecular structure is achieved by the proper balance of attractive (ion-dipole, H-bonding, dipole-dipole, and π-π) and the repulsive interactions (steric and electronic effects).

Previously reported **mAG**–based assemblies[23] showed promising characteristics for the construction of SADs such as, respectively: 32 and 64 hydroxyls at the end groups and molecular weights of 12.4 and 16.1 kDa.[24] Yet, neither $\mathbf{1}_{16}$ nor $\mathbf{2}_{16}$ had large enough dendrons to reach a fractal geometry characteristic of high-generation dendrimers. Furthermore, would the SAD form and be reasonably stable even with the increased steric hindrance? If it did, what would the structure and stability of the resulting system be? In here we report the answer to those question.[25]

In order to test the tolerance of the **mAG** motif, to the size of the moieties attached to the sugar, we constructed **3** having sixteen hydroxyls in each dendron and a molecular weight of 2.4 kDa (Scheme 1, Figure S1).[26] The covalent synthesis of the dendronized **mAG** derivate **3** was achieved as reported previously for **1** and **2**.[24] The insertion of bis-(MPA) dendrimer was made via the copper-catalyzed Huisgen cycloaddition of the corresponding Dg_3 alkyne and **mAG**haz (Scheme 1). The identity and purity of **3** was assessed using a combination of techniques such as ESI-MS, ^{1}H-NMR, ^{13}C-DEPTQ-NMR, and IR (Figures S1-S3).[26]

Experimental

Materials

Polyester-8-hydroxyl-1-acetylene bis MPA dendron, generation 3 was used as purchased from Sigma-Aldrich. All other reagents were obtained from commercial sources and used without further purification. Unless otherwise noted, all compounds were purified by column chromatography on silica gel 60, 0.04-0.063 mm, and TLC and PTLC (from Sorbent Technologies) were performed using EMD silica gel 60 F_{254} glass backed plates from Sorbent Technologies. Visualization of spots was achieved with UV radiation, iodine, and/or by staining with either 3,5-dinitrophenylhydrazine or phosphomolybdic acid in ethanol. Reactions requiring anhydrous conditions were carried out using flame-dried glassware under Argon.

Characterization

^{1}H and ^{13}C NMR spectra were recorded on Bruker DRX-500 (TopSpin v 2.0) with nominal frequencies of 500.1 MHz for proton or 125.8 MHz for carbon, respectively. ^{1}H NMR and ^{13}C NMR chemical shifts are reported in parts per million (ppm) relative to the residual undeuterated solvent as an internal reference. *Sodium 3-(trimethylsilyl)propionate-2,2,3,3-d_4*

(Sigma-Aldrich) was used as the internal standard for the NMR experiments performed in D_2O or H_2O:D_2O (9:1). All the NMR experiments were performed at 298.2 K unless otherwise stated. The following abbreviations are used to describe the multiplicities: s, singlet; d, doublet; t, triplet; q, quartet; m, multiplet; br, broad. High-resolution mass spectral data were obtained from Emory University Mass Spectrometry Center using a Micromass VG AutoSpec magnetic sector mass spectrometer (70 eV). FT-IR analyses were performed in a Bruker Tensor 27 Infrared Spectrometer equipped with a Helios Attenuated Total Reflectance (ATR) accessory containing a diamond crystal. Melting temperatures were determined using a Fisher brand electro-thermal digital melting point apparatus (Fisher Scientific).

Synthesis of 3

To a suspension of alkyne-Dg_3 (250 mg, 288 mmol) and **mAG**haz (90 mg, 135 mmol)[24] in THF:phosphate buffer (5 mL; pH 7.0; 3:1) were added sodium ascorbate (15% mol) and $CuSO_4 \cdot 5H_2O$ (5% mol). The reaction mixture was then allowed to stir at room temperature until completion as determined by TLC (CH_2Cl_2:MeOH; 80:20). The solvents were evaporated and the crude product was purified by dry-loading of a silica column followed by flash chromatography eluted with dichloromethane and gradually increasing the polarity with methanol (up to 25%). The fractions containing product were combined, the solvent removed and the resulting solid further washed three times with acetonitrile (<1%) in hexanes to give **3** (59%, 194 mg, 80 mmol) as a white foam (purity > 95% as determined by NMR). mp 249.5-255.5 °C (decomposition). ^{1}H NMR (500 MHz, DMSO-d_6): δ 10.95 (s, 2H), 8.20 (s, 2H), 8.13 – 8.03 (m, 6H), 7.89 (d, *J* = 7.7 Hz, 2H), 7.69 (t, *J* = 7.7 Hz, 2H), 7.28 (s, 1H), 6.71 – 6.62 (m, 2H), 6.57 (s, 3H), 6.10 (t, *J* = 6.9 Hz, 2H), 5.44 (s, 2H), 5.16 (s, 8H), 4.65 (s, 31H), 4.44 (d, *J* = 7.2 Hz, 2H), 4.28 (dd, *J* = 9.2 Hz, 16.1 Hz, 10H), 4.16 (dt, *J* = 11.9 Hz, 23.8 Hz, 20H), 4.09 (t, *J* = 9.1 Hz, 31H), 3.53 (s, 2H), 3.42 (dd, *J* = 10.1 Hz, 27.8 Hz, 69H), 2.63 (s, 6H), 2.39 – 2.32 (m, 2H), 2.32 – 2.23 (m, 8H), 2.20 (s, 2H), 2.07 (s, 9H), 1.82 – 1.72 (m, 13H), 1.62 (s, 2H), 1.52 (d, *J* = 8.2 Hz, 8H), 1.39 (s, 1H), 1.22 (d, *J* = 7.2 Hz, 9H), 1.17 (s, 13H), 1.10 (s, 24H), 1.00 (s, 50H), 0.87 (s, 2H) (Figure S2). ^{13}C NMR (125.8 MHz, DMSO-d_6) δ 197.5, 174.4, 174.3, 174.1, 172.6, 172.4, 171.8, 156.7, 153.3, 152.0, 146.1, 141.4, 141.3, 137.1, 133.3, 130.5, 129.2, 128.9, 128.8, 124.7, 117.2, 84.7, 81.8, 74.6, 64.5, 63.7, 63.4, 60.2, 58.1, 57.9, 50.3, 49.2, 46.3, 46.2, 40.2, 40.1, 40.0, 39.8, 39.7, 39.5, 39.3, 39.2, 39.0, 34.0, 33.12, 33.1, 29.4, 29.4, 29.3, 28.1, 26.8, 26.4, 25.3, 25.3, 23.7, 23.7, 22.5, 17.0, 16.7, 1.2. (Figure S3) IR (νmax): 3357, 2942, 2883, 1728, 1684, 1469, 1573, 1371, 1293, 1221, 1123, 1039, 659, 533 cm^{-1}. HRMS (m/z): $[M+1]^+$ calcd 2401.0103 for $C_{106}H_{157}N_{11}O_{51}$; found 2401.0105 (Figure S1).

Self-Assembly Studies

The self-assembly studies were performed using a Bruker DRX-500 NMR spectrometer, equipped with a 5 mm BBO probe. For the NMR measurements in water we used a conventional 1D presaturation pulse sequence with the excitation pulse set over the water peak at 4.7 ppm. Solutions of **3** (10 mM, 600 μL) in 0.1 PBS, pH 7.1 in H_2O-D_2O (9:1) were used. For the NOESY experiment, a phase-sensitive 2D NOESY pulse sequence with presaturation (noesyphpr) was used (Figure S4-S5).[26]

Pulsed Field Gradient NMR (PFG-NMR)

Diffusion experiments were carried out with a Bruker DRX-500 spectrometer equipped with a 5 mm BBO probe and using the Stimulated Echo Pulse Gradient sequence (stebpgp1s) in FT mode. To improve homogeneity a “13 interval pulse sequence” was used with two pairs of bipolar gradients. The sine-shaped gradient was used and the temperature was actively controlled at 25.0 ± 0.5 °C. Diffusion coefficients were derived using integration of the desired peaks to a single exponential decay, using the Bruker software package T1/T2

Relaxation (TopSpin v 2.0). Calculation of the hydrodynamic radius in D_2O used the viscosity value (η = 1.103 Kg m^{-1} s^{-1}, 298.15 K) reported in the literature.[27] The hydrodynamic radii of the species in the NMR tube were calculated according to the spherical approximation using the Einstein-Stokes equation:

$$D=\frac{k_B T}{6\pi\eta r_H}$$

where T denotes the temperature, η is the viscosity of the solvent at the given temperature, k_B is the Boltzmann-Constant, D is the measured diffusion constant and r_H is the hydrodynamic radius. The data were further processed by the Bruker software package.

Dynamic Light Scattering (DLS)

DLS measurements were performed in a DynaPro Titan (Wyatt Technology Corporation) with temperature control (25 °C) and a microsampler with a diode laser at a scattering angle of 90°, a wavelength at 657 nm, and a power of 15 mW. The measurements were performed using solutions of **3** (10 mM) dispersed in a PBS solution (0.1 M, pH 7.1) and filtered with a 0.45 μm Nylon filter (Fisher brand, 10 mm o.d. glass tubes) prior to all DLS measurements. (See Table 1, Graph S1-S3)

Computational Analysis

Molecular models of $\mathbf{1}_{16}$ and $\mathbf{3}_{16}$ were constructed and minimized using MacroModel representing water as a continuum solvent.[28] The hydrodynamic radii (r_H) were calculated by averaging seven measurements starting from the central cation to the terminal groups with the error reported as the standard deviation. The resulting calculated hydrodynamic radii (r_H) for $\mathbf{1_{16}}$ and $\mathbf{3_{16}}$ were 2.5 nm and 2.9 nm respectively (Figure S6).[26]

Variable Temperature ^{1}H NMR

A solution of $\mathbf{3}_{16}$ (10 mM) in PBS (0.1 M, pH 7.1, 3 M KI) was placed in a threaded cap sealed NMR tube. The ^{1}H-NMR was recorded in H_2O-D_2O (9:1) in the range of 25-80 °C in increments of 5 °C or 10 °C. The T_m is defined as the temperature at which there is a 1:1 ratio of $\mathbf{3}_{16}$:**3** as determined by the average of the integrations of four peaks corresponding to the protons of each species at: 8.0 ppm, 7.8 ppm, 7.6 ppm, and 6.5 ppm.

Results and discussion

Self-assembly studies

Self-assembly studies were performed by adding KI (3 M) to a suspension of **3** (10 mM in a H_2O:D_2O (9:1) phosphate buffered saline (PBS, 0.1 M, pH 7.1)) and letting the sample equilibrate overnight in a shaker after which time the solution becomes clear and homogenous. The sample was analyzed by ^{1}H-NMR and 2D NOESY using presaturation pulse sequence (Figure S4-S5,[26] Figure 1c). ^{1}H NMR experiments of $\mathbf{3}_{16}$ reveal the signatures for its self-assembly in aqueous media.[21] The ^{1}H NMR spectrum shows the hexadecamer's characteristic double set of signals at 12.8 ppm and 11.3 ppm (Figures 1c and S4) corresponding to two pairs of tetrads in different chemical environments (Figure 1b). The 2D NOESY spectrum supports the formation of $\mathbf{3}_{16}$, by showing the signature cross peaks distinctive of a hexadecamer in water (Figure 1b, 1c).[21]

Size and molecular weight

Assembly $\mathbf{3}_{16}$ has a molecular weight of 38.9 kDa and 256 hydroxyls as end groups. The size of $\mathbf{3}_{16}$ was measured by both Pulse Field Gradient-NMR (PFG-NMR), and Dynamic Light Scattering (DLS) using very similar conditions to those used in the NMR experiments. The calculated diameters (D_H) by PFG-NMR and DLS experiments are in good agreement with each other giving values of (4.8 ± 0.8) nm and (5.3 ± 0.1) nm, respectively.(See supp. Table S1, Graph S1-S3) A molecular model constructed and minimized, using a continuum solvation model for water,[28] provides a diameter of (5.8 ± 0.8) nm (Figures 2b, S6).[26] The size discrepancies between the values calculated by molecular modeling and those determined experimentally are likely from limitations in the modeling protocol (e.g., shortcomings in the solvation model). The minimizations were performed using a low ionic strength solvation model whereas the PFG-NMR and DLS experiments were performed in PBS (0.1 M) containing KI (3 M). The average diameter for $\mathbf{3}_{16}$ (from PFG-NMR and DLS measurements) was 5.0 nm with that for its lower generation congeners $\mathbf{1}_{16}$ and $\mathbf{2}_{16}$ being 4.3 nm and 4.5 nm, respectively.[24] It is evident that an increase in the dendron generation, and concomitant increase in molecular weight, does not lead to a proportional increase the size of the resulting SAD. This is characteristic of the fractal geometry of higher generation dendrimers in which the size increases slower than the density.[2,29] Dendrimers of higher generations are described as having a fractal geometry if they have a particular property (e.g., topology, pattern of connectivity) that shows “scale-invariance” or “self-similarity”.[2] The fractal geometry of $\mathbf{3}_{16}$ is evident in Figure 2 where its solvent accessible surface area is more congested than that of $\mathbf{1}_{16}$. Other consequences of reaching this fractal geometry is the increase in surface irregularity, or complexity, and the formation of void spaces with potential for encapsulating smaller guest molecules.

Thermal stability studies

Variable temperature (VT) NMR experiments were performed to assess the thermodynamic stability of $\mathbf{3}_{16}$, using identical conditions to the previously described assembly studies (Figure 3). A concentration of 10 mM in **3** offers a good proportion of monomer to assembly $\mathbf{3}_{16}$, enabling a determination of a melting temperature (T_m, defined here as the temperature at which the ratio $\mathbf{3}_{16}$:**3** is 1:1) by integration of the peaks corresponding to both species (Figure S7).[22,26] These experiments show that the steric bulk within $\mathbf{3}_{16}$ induce a slight decrease in the thermodynamic stability (T_m = 68 °C),[26] when compared to its lower generation congeners ($\mathbf{1}_{16}$, T_m = 77 °C; $\mathbf{2}_{16}$, T_m = 72 °C)[24] (Table 1). Nevertheless, the decrease in stability is relatively small, with a significant amount of $\mathbf{3}_{16}$ (19%) still present at 80 °C (Figure 3). This remarkable stability might reflect the antagonistic effects within $\mathbf{3}_{16}$. On one hand, it is energetically more costly to bring sixteen sterically bulky subunits close to each other. On the other hand, the protected microenvironment created by the dendrons should shield the core from detrimental interactions with the solvent molecules, in addition to the potential to establish other stabilizing van der Waals interactions between the dendrons.

Conclusions

To the best of our knowledge $\mathbf{3}_{16}$ is the first reported discrete and water soluble SAD with the largest molecularity. The versatility of this approach for the construction of dendrimers of sizes akin to soluble proteins[1] is illustrated by the fact that $\mathbf{3}_{16}$ display 256 hydroxyls at the end groups. By comparison, to achieve an equivalent architecture with a fully covalent dendrimer will require, for example, the synthesis and coupling of four sixth-generation dendrons to a tetrafunctional core.[30] Moreover, in addition to being discrete and water soluble, this family of SADs $(\mathbf{1}\text{-}\mathbf{3})_{16}$ are: well defined, relatively easy to make, chiral, thermally stable, and possess a functional core (suitable for the encapsulation of guest

molecules such as drugs).[31,32] The fact that these SADs are held together by multiple noncovalent interactions enables the fine-tuning of their structure and dynamics by using a wide variety of external stimuli. The use of polyester dendrons also increases the chances for these SADs to be biocompatible. We are currently evaluating the use of these and related systems in the development of dendritic molecular containers and multifunctional probes.

Supplementary Material

Refer to Web version on PubMed Central for supplementary material.

Acknowledgments

This research was financially supported by the NIH-SCoRE (SC1GM093994) and NIH-NCRR (P20 RR016470). For graduate fellowships L.R.R. thanks the UPR Golf Fellowship Program and J.E.B. thanks the Alfred P. Sloan Foundation and NSF-IFN-EPSCoR (01A-0701525).

References

1. Goodsell DS, Olson AJ. Trends Biochem. Sci 1993;18:65–68. [PubMed: 8480362]
2. Newkome, GR.; Moorefield, CN.; Vogtle, F. Dendritic Molecules: Concepts, Synthesis, Perspectives. VCH Publisher; New York: 1996.
3. (a) Zeng FW, Zimmerman SC. Chem. Rev 1997;97:1681–1712. [PubMed: 11851463] (b) Zimmerman SC, Zeng FW, Reichert DEC, Kolotuchin SV. Science 1996;271:1095–1098. [PubMed: 8599085]
4. Tekade RK, Kumar PV, Jain NK. Chem. Rev 2009;109:49–87. [PubMed: 19099452]
5. Astruc D, Boisselier E, Ornelas C. Chem. Rev 2010;110:1857–1959. [PubMed: 20356105]
6. Bi S, Hao S, Li L, Zhang S. Chem. Commun 2010;46:6093–6095.
7. Crespo L, Sanclimens G, Pons M, Giralt E, Royo M, Albericio F. Chem. Rev 2005;105:1663–1681. [PubMed: 15884786]
8. Zhuravel MA, Davis NE, Nguyen ST, Koltover I. J. Am. Chem. Soc 2004;126:9882–9883. [PubMed: 15303837]
9. Boas U, Christensen JB, Heegaard PMH. J. Mater. Chem 2006;16:3785–3798.
10. (a) Roy R, Kim JM. Tetrahedron 2003;59:3881–3893. (b) Zheng Y-R, Ghosh K, Yang H-B, Stang PJ. Inorg. Chem 2010;49:4747–4749. [PubMed: 20443570] (c) Yang H-B, Das N, Huang F, Hawkridge AM, Muddiman DC, Stang PJ. J. Am. Chem. Soc 2006;128:10014–10015. [PubMed: 16881621]
11. Joester D, Losson M, Pugin R, Heinzelmann H, Walter E, Merkle HP, Diederich F. Angew. Chem. Int. Ed 2003;42:1486–1490.
12. Giles MD, Liu S, Emanuel RL, Gibb BC, Grayson SM. J. Am. Chem. Soc 2008;130:14430–14431. [PubMed: 18847205]
13. Corbellini F, Di Costanzo L, Crego-Calama M, Geremia S, Reinhoudt DN. J. Am. Chem. Soc 2003;125:9946–9947. [PubMed: 12914457]
14. Rosen BM, Wilson CJ, Wilson DA, Peterca M, Imam MR, Percec V. Chem. Rev 2009;109:6275–6540. [PubMed: 19877614]
15. Smith DK, Hirst AR, Love CS, Hardy JG, Brignell SV, B. H. Prog. Polym. Sci 2005;30:220–293.
16. Hunter CA, Tomas S. J. Am. Chem. Soc 2006;128:8975–8979. [PubMed: 16819894]
17. Oshovsky GV, Reinhoudt DN, Verboom W. Angew. Chem., Int. Ed 2007;46:2366–2393.
18. Davis JT, Spada GP. Chem. Soc. Rev 2007;36:296–313. [PubMed: 17264931]
19. Davis JT. Angew. Chem., Int. Ed 2004;43:668–698.
20. Gubala V, Betancourt JE, Rivera JM. Org. Lett 2004;6:4735–4738. [PubMed: 15575673]
21. García-Arriaga M, Hobley G, Rivera JM. J. Am. Chem. Soc 2008;130:10492–10493. [PubMed: 18642917]
22. Betancourt JE, Rivera JM. Org. Lett 2008;10:2287–2290. [PubMed: 18452304]

23. The nomenclature for such derivatives is $mAGD_X(OH)_{2x}$, where X = 1 (**1**), 2 (**2**), 4 (**3**) with the corresponding assemblies $[mAGD_X(OH)_{2x}]_{16}$•3KI abbreviated as $\mathbf{1}_{16}$, $\mathbf{2}_{16}$, or $\mathbf{3}_{16}$ throughout the article.
24. Betancourt JE, Rivera JM. J. Am. Chem. Soc 2009;131:16666–16668. [PubMed: 19883053]
25. The effects of steric hindrance on the self-assembly was first discuss by Whitesides in the context of cyclic vs. linear self-assembly: (a) Zerkowski JA, Whitesides GM. J. Am. Chem. Soc 1994;116:4298–4304. (b) Mathias JP, Simanek EE, Whitesides GM. J. Am. Chem. Soc 1994;116:4326–4340. In the context of dendrimers, these effects were later investigated by Zimmerman and co-workers in: Ma Y, Kolotuchin SV, Zimmerman SC. J. Am. Chem. Soc 2002;124:13757–13769. [PubMed: 12431106]
26. See Supporting Information.
27. Harris KR, A. WL. J. Chem. Eng. Data 2004;49:1064–1069.
28. Minimizations were performed using OPLS2005* (MacroModel) Version 9.5, Maestro 8.0.315. Schrödinger, LLC; New York: 2007. with water represented as a continuum solvent
29. Ballauff M, Likos CN. Angew. Chem., Int. Ed 2004;43:2998–3020.
30. To calculate the number of surface or end groups (*Z*) one can use the formula $Z = N_c N_b{}^G$, where N_c is the branching of the core, N_b is the branching of the repeat unit (two for the bifunctional bis-MPA), and G is the generation number. For $\mathbf{3}_{16}$, $Z = (16)(2)^4 = 256$, and for a hypothetical covalent dendrimer using a tetrafunctional core and a sixth generation bifunctional repeat unit, $Z = (4)(2)^6 = 256$. For more details see reference [1].
31. Smith DK, Diederich F. Chem. Eur. J 1998;4:1353–1361.
32. Diederich F, Felber B. Proc. Natl. Acad. Sci. U.S.A 2002;99:4778–4781. [PubMed: 11891306]

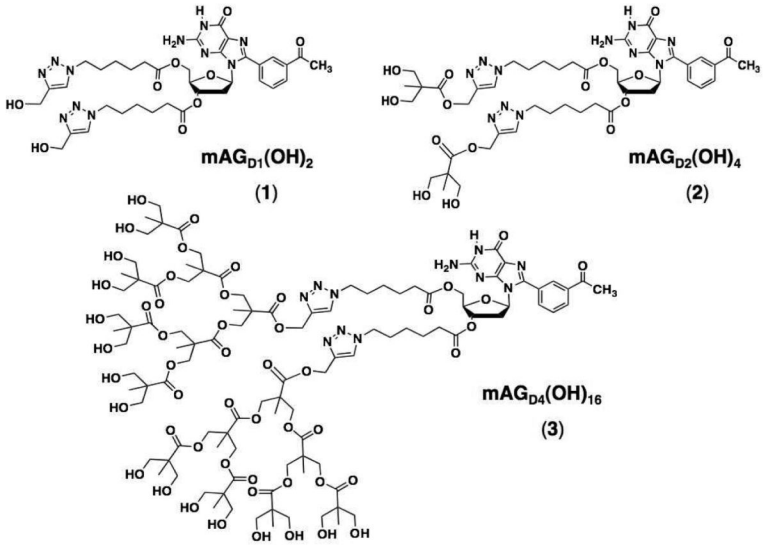

Chart 1.
Line structures of **1, 2** and **3**.[24]

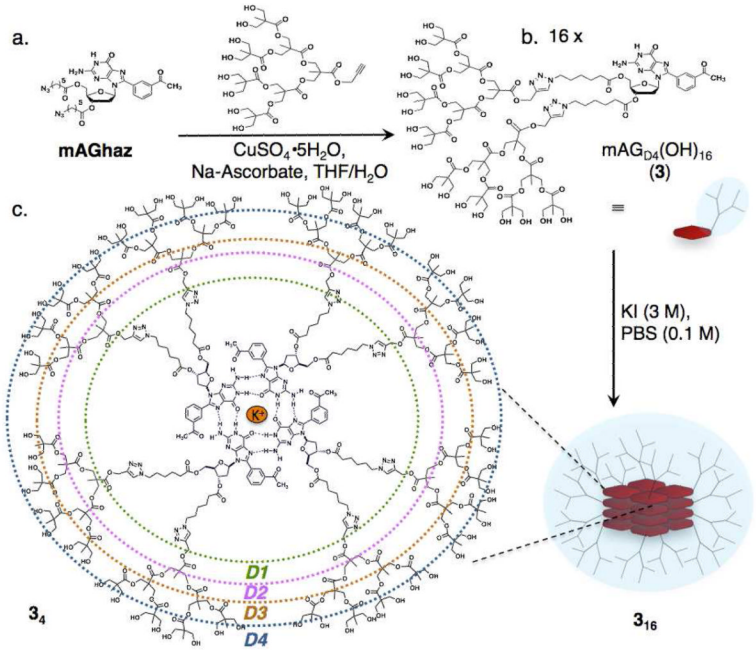

Scheme 1.

(a) Covalent synthesis of **3** via the key step of a copper-catalyzed Huisgen cycloaddition. (b) Self-assembly of hexadecameric dendrimer by the addition of the potassium cation template. (c) Line structure of a tetrad of **3**, where the colors represent the different dendritic generations: green, D1; pink, D2; orange, D3; blue, D4.

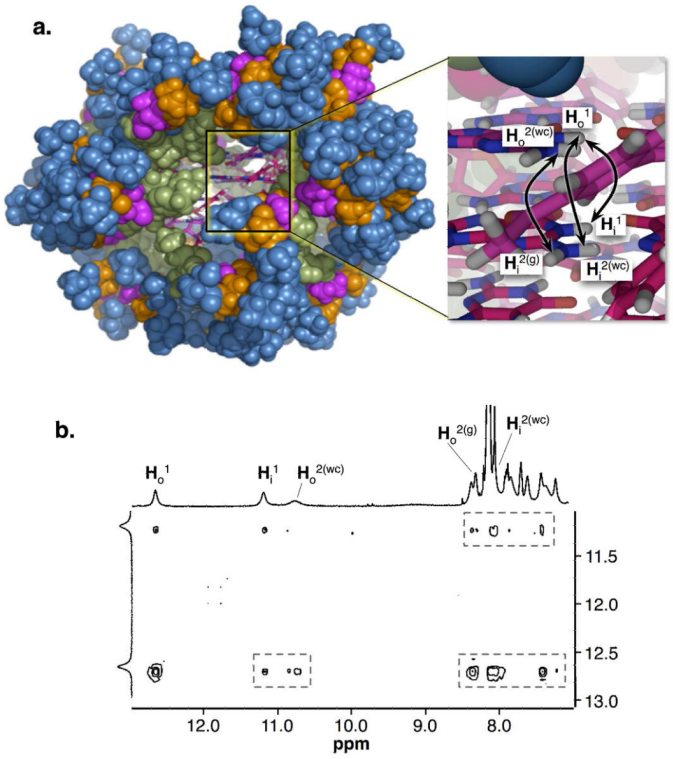

Figure 1.

(a) Molecular model of $\mathbf{3}_{16}$ constructed and minimized using MacroModel[28] (the colors represent the different dendritic generations: green, D1; pink, D2; orange, D3; blue, D4). The inset shows a close up of the core of the assembly (carbons are shown in pink; oxygens in red; hydrogens in white; nitrogens in blue). The the double point arrows indicate to selected NOE interactions that give rise to the hexadecamer signature cross peaks. (b) 2D NOESY (500 MHz) showing a series of signature cross peaks that support the the structure of $\mathbf{3}_{16}$ (Figure S5).[21,26]

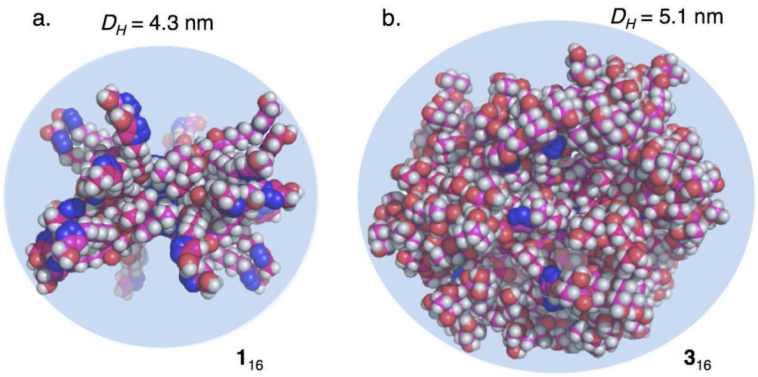

Figure 2.

Molecular models of (a) $\mathbf{1}_{16}$ and (b) $\mathbf{3}_{16}$ minimized using a continuum solvation model for water.[28] Carbons are shown in pink, oxygens in red, hydrogens in white, and nitrogens in blue. The reported diameters are the average of the values determined by PFG-NMR and DLS.

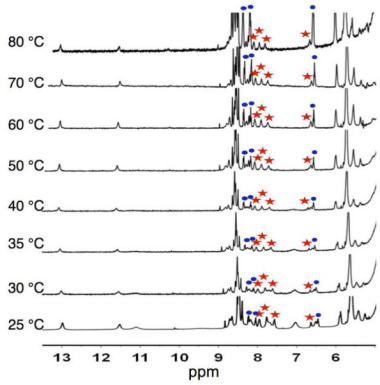

Figure 3.

Variable temperature (VT) ^{1}H NMR (500 MHz) spectra for $\mathbf{3}_{16}$ in H_2O-D_2O (9:1; 10 mM in **3**; 3 M KI; 0.1 M PBS; pH 7.1). The amounts of $\mathbf{3}_{16}$ as a function of temperature are (from bottom to top): 75%, 68%, 69%, 59%, 63%, 61%, 45%, and 19%. The percentage of assembly ($\mathbf{3}_{16}$) were calculated from the average values obtained by integrating the marked peaks corresponding to $\mathbf{3}_{16}$ (red stars) and **3** (blue circles).[26]

Table 1

Summary of results for $\mathbf{1}_{16}$ and $\mathbf{3}_{16}$. Molecular weight (MW); diffusion coefficients (D) and hydrodynamic diameter (D_H) by PFG-NMR in H_2O-D_2O (9:1); D_H by DLS (Table S1, Graph S1-S3, all at 10 mM in **3**; 3 M KI; 0.1 M PBS; pH 7.1); measured D_H of the minimized MacroModel structure[27] (Figure S6) and T_m values (Figure S7).[26]

SAD	MW (kDa)	PFG-NMR $D \times 10^{11}$ (m^2 s^{-1}) at 25 °C	D_H (nm)			T_m (°C)
			PFG-NMR	DLS	Modeling	
$\mathbf{1}_{16}$	12.90	9.3 ± 0.3	4.3 ± 0.1	4.2 ± 0.4	4.8 ± 0.4	77
$\mathbf{3}_{16}$	38.92	8.4 ± 1.2	4.8 ± 0.8	5.3 ± 0.1	5.8 ± 0.4	68